

Time-VLM: Exploring Multimodal Vision-Language Models for Augmented Time Series Forecasting

Siru Zhong¹ Weilin Ruan¹ Ming Jin² Huan Li³ Qingsong Wen⁴ Yuxuan Liang¹

Abstract

Recent advancements in time series forecasting have explored augmenting models with text or vision modalities to improve accuracy. While text provides contextual understanding, it often lacks fine-grained temporal details. Conversely, vision captures intricate temporal patterns but lacks semantic context, limiting the complementary potential of these modalities. To address this, we propose Time-VLM, a novel multimodal framework that leverages pre-trained Vision-Language Models (VLMs) to bridge temporal, visual, and textual modalities for enhanced forecasting. Our framework comprises three key components: (1) a Retrieval-Augmented Learner, which extracts enriched temporal features through memory bank interactions; (2) a Vision-Augmented Learner, which encodes time series as informative images; and (3) a Text-Augmented Learner, which generates contextual textual descriptions. These components collaborate with frozen pre-trained VLMs to produce multimodal embeddings, which are then fused with temporal features for final prediction. Extensive experiments across diverse datasets demonstrate that Time-VLM achieves superior performance, particularly in few-shot and zero-shot scenarios, thereby establishing a new direction for multimodal time series forecasting.

1. Introduction

Time series forecasting plays a pivotal role across numerous domains, including finance (Idrees et al., 2019), climate (Karevan & Suykens, 2020), energy (Deb et al., 2017), and transportation (Zheng & Huang, 2020). Accurate predictions of future trends enable better decision-making, risk management, and resource allocation. Traditional statistical models, like ARIMA, have been the go-to methods for time series analysis, but they often struggle to capture complex,

¹The Hong Kong University of Science and Technology (Guangzhou)²Griffith University³Zhejiang University⁴Squirrel AI. Correspondence to: Yuxuan Liang <yuxliang@outlook.com>.

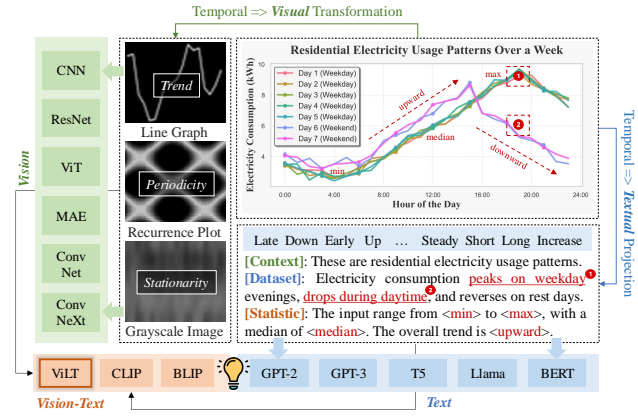


Figure 1: Our Time-VLM combines text (Right) and vision (Left) modalities to augment time series forecasting.

non-linear dependencies in large datasets. In contrast, deep learning approaches, e.g., RNNs (Medsker et al., 2001) and Transformer-based models (Li et al., 2019; Wu et al., 2021; Zhou et al., 2021; Liu et al., 2022a; Zhou et al., 2022; Nie et al., 2023), have revolutionized this field by learning intricate temporal patterns from raw data through techniques such as patch-based restructuring, auto-correlation mechanisms, and frequency decomposition strategies, delivering superior performance across various forecasting tasks. However, these models often struggle with domain generalization and scenarios with limited training data, particularly in few/zero-shot settings (Liang et al., 2024).

To overcome these issues, researchers have turned to *augmenting time series forecasting with additional modalities*, such as *text* and *images*, which provide complementary information that can enhance predictive accuracy:

- **Text-Augmented Models:** Textual data, such as task-specific knowledge or domain events, provides valuable context for time series forecasting. For example, in financial forecasting, market descriptions or policy changes can enhance accuracy by adding insights beyond raw data. Approaches like Time-LLM (Jin et al., 2024) and UniTime (Liu et al., 2024b) map time series into textual representations, leveraging Large Language Models (LLMs) to capture contextual influences and infer predictions (Figure 1, right). However, these models face two challenges: (1) the *modality gap* between continuous time series and

discrete text leads to information loss, and (2) pre-trained word embeddings are rarely optimized for time series forecasting, limiting fine-grained temporal pattern capture.

- **Vision-Augmented Models:** In contrast, transforming time series data into visual representations, such as through Gramian Angular Fields (GAF) or recurrence plots, enables models to identify and exploit underlying visual patterns, thereby facilitating the extraction of intricate temporal relationships using image-based feature learning techniques (e.g., CNNs) (Figure 1, left). Recent work (Wu et al., 2023b; Wang et al., 2024; Chen et al., 2024) demonstrates the natural alignment between time series and vision, as both are continuous and share structural similarities, allowing pretrained vision models to effectively extract hierarchical temporal features. However, these models often lack semantic context, limiting their ability to capture domain-specific knowledge or event-driven insights critical for real-world forecasting.

Despite advancements in text- and vision-based models, integrating both modalities with time series remains underexplored. Vision-Language Models (VLMs) (Radford et al., 2021) excel in aligning vision and text for tasks like multimodal reasoning. Building on this, we introduce Time-VLM, extending VLMs to include time series as a third modality. Each modality—text for semantic context, vision for spatial patterns, and time series for temporal dynamics—offers unique strengths. Current approaches often focus on single modalities, limiting their ability to harness the complementary benefits of all three. Our method leverages pretrained VLMs to effectively integrate temporal, visual, and textual data for augmented time series forecasting.

By projecting time series into a unified vision-language semantic space, Time-VLM enables rich cross-modal interactions, combining the strengths of both modalities while mitigating their individual limitations. Specifically, Time-VLM introduces three key components: (1) a *Retrieval-Augmented Learner* that processes raw time series data through patch-based feature extraction and memory bank interactions to generate enriched temporal representations, capturing both local and global dependencies; (2) a *Vision-Augmented Learner* that adaptively transforms time series into images using multi-scale convolution, frequency encoding, and periodic encoding, preserving both fine-grained details and high-level structures; and (3) a *Text-Augmented Learner* that generates rich textual context (e.g., statistics and dataset descriptions) to complement the visual representations. These modules collaborate with VLMs to integrate temporal, visual, and textual modalities, producing accurate forecasts through a fine-tuned predictor.

Our key contributions are summarized as follows:

- We propose the first framework unifying temporal, visual,

and textual modalities via pretrained VLMs, complementing their strengths for augmented time series forecasting.

- We introduce three components: a Retrieval-Augmented Learner for temporal feature enhancement via memory bank interactions, a Vision-Augmented Learner for adaptive time-series-to-image transformation, and a Text-Augmented Learner for contextual prompt generation.
- Time-VLM achieves superior performance, particularly in few-shot and zero-shot scenarios, establishing a new direction for multimodal time series forecasting.

2. Related Work

Text-Augmented Models for Time Series Forecasting.

The success of LLMs inspires their application to time series tasks. Methods like LLMTIME (Gruver et al., 2023) and LLM4TS (Chang et al., 2023) tokenize time series data for autoregressive prediction but inherit LLMs’ limitations, such as poor arithmetic and recursive capabilities. Recent approaches, including GPT4TS (Zhou et al., 2023) and TimeLLM (Jin et al., 2024), project time series into textual representations to leverage LLMs’ reasoning abilities. However, they face challenges like the modality gap and lack of time series-optimized word embeddings, leading to potential information loss. UniTime (Liu et al., 2024b) and TimeFFM (Liu et al., 2024a) incorporate domain-specific instructions and federated learning, respectively, but remain constrained by their reliance on text alone.

Vision-Augmented Models for Time Series Forecasting.

Vision emerges as a natural way to preserve temporal patterns. Early approaches use CNNs for matrix-formed time series (Li et al., 2020; Sood et al., 2021), while TimesNet (Wu et al., 2023b) introduces multi-periodic decomposition for unified 2D modeling. VisionTS (Chen et al., 2024) pioneers pre-trained visual encoders with grayscale time series images, and TimeMixer++ (Wang et al., 2024) advances the field with multi-scale frequency-based time-image transformations. Despite their effectiveness in temporal modeling, these methods often lack semantic context, hard to use high-level contextual information for prediction.

Vision-Language Models.

VLMs like ViLT (Kim et al., 2021), CLIP (Radford et al., 2021), and ALIGN (Jia et al., 2021) transform multimodal understanding by aligning visual and textual representations. Recent advancements, like BLIP-2 (Li et al., 2023) and LLaVA (Liu et al., 2023), further enhance multimodal reasoning. However, VLMs remain underexplored for time series analysis. Our work bridges this gap by leveraging VLMs to integrate temporal, visual, and textual modalities, addressing the limitations of unimodal approaches.

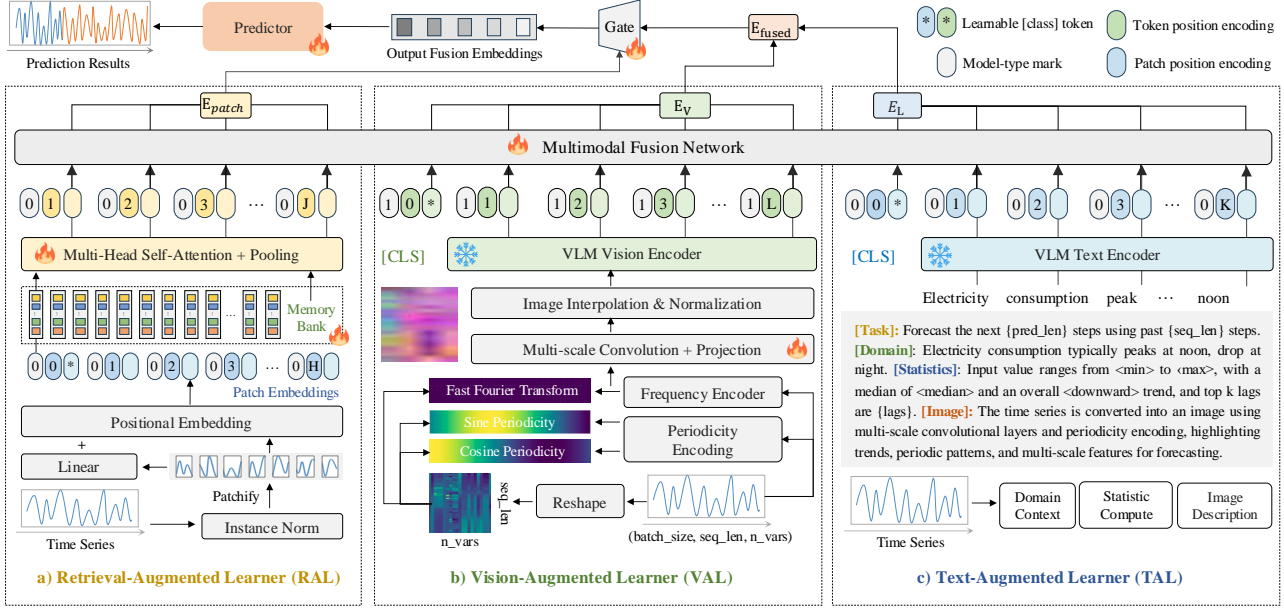


Figure 2: Overview of the Time-VLM framework.

3. Methodology

To address the limitations of single-modality approaches and leverage the complementary strengths of visual, textual, and temporal modalities, we propose Time-VLM, a unified framework that integrates these modalities for enhanced time series forecasting. As illustrated in Figure 2, the framework comprises three core components:

- **Retrieval-Augmented Learner (RAL):** Extracts temporal features from raw time series patches, maintains a memory bank to interact with patch embeddings via multi-head self-attention and pooling mechanisms, preserving rich temporal feature representations and enhancing long-term dependency modeling for robust forecasting.
- **Vision-Augmented Learner (VAL):** Transforms time series into informative three-channel images through multi-scale convolutions, frequency and periodic encoding. The images are processed by a frozen VLM vision encoder to extract hierarchical visual features, capturing both fine-grained details and high-level temporal patterns.
- **Text-Augmented Learner (TAL):** Generates contextual textual prompts for the input time series, including statistical features (e.g., mean, variance, trends), domain-specific context (e.g., electricity consumption patterns), and image descriptions. These prompts are encoded by a frozen VLM text encoder to produce textual embeddings.

The image and text embeddings, extracted by the VLM, are integrated with temporal memory features via a gated fusion mechanism, effectively capturing complementary information to improve forecasting accuracy. These enriched multimodal features are then processed by a fine-tuned predictor to generate precise and reliable forecasts.

3.1. Retrieval-Augmented Learner (RAL)

The RAL module extracts high-level temporal features via patch-based processing and memory-enhanced attention. It dynamically retrieves and integrates temporal patterns, adapting to complex time series structures to enhance forecasting performance. It operates in two key stages.

Patch Embedding: The input time series $x_{enc} \in \mathbb{R}^{B \times L \times D}$ (batch size B , sequence length L , variables D) is divided into overlapping patches of length $patch_len$ with stride $stride$. Each patch is projected into a d_{model} -dimensional space via a linear layer, and positional embeddings are added to preserve temporal order. The resulting patch embeddings $E_{patch} \in \mathbb{R}^{B \times (D \cdot N_{patches}) \times d_{model}}$ capture local temporal patterns, where $N_{patches}$ is the number of patches.

Memory-Enhanced Attention: A set of learnable memory queries $Q \in \mathbb{R}^{N_{queries} \times d_{query}}$ interact with patch embeddings through multi-head attention. Patch embeddings are projected into keys K and values V , computing:

$$\text{Memory}(Q, K, V) = \text{softmax} \left(\frac{QK^\top}{\sqrt{d_{query}}} \right) V. \quad (1)$$

To better capture complex temporal dynamics, we introduce a hierarchical memory structure with two levels:

- **Local Memory:** Captures fine-grained patterns within individual patches for short-term dependencies.
- **Global Memory:** Aggregates information across patches for long-range dependencies and high-level trends.

The two memories are fused via a gated mechanism:

$$M_{\text{fused}} = \alpha \cdot M_{\text{local}} + (1 - \alpha) \cdot M_{\text{global}}, \quad (2)$$

where α is a learnable gating parameter that adaptively balances the contribution of local and global memory.

The output $\mathbb{R}^{B \times N_{\text{queries}} \times d_{\text{query}}}$ stores high-level temporal patterns, enabling dynamic retrieval and fusion with other modalities. Each memory slot captures semantic and temporal relationships, allowing adaptive retrieval relevant patterns based on the input context. This hierarchical memory mechanism effectively addresses challenges in capturing long-range dependencies and complex temporal dynamics.

3.2. Vision-Augmented Learner (VAL)

The VAL module adaptively transforms time series $x_{\text{enc}} \in \mathbb{R}^{B \times L \times D}$ into images, preserving both fine-grained and high-level temporal patterns through following operations:

Frequency and Periodicity Encoding: To capture spectral and temporal dependencies, the VAL module applies two complementary encoding techniques to the input time series, explicitly add frequency and time-domain information.

1. Frequency Encoding: A Fast Fourier Transform (FFT) extracts frequency components as:

$$\text{FFT}(x_{\text{enc}}) = \sum_{t=0}^{L-1} x_{\text{enc}}(t) \cdot e^{-2\pi i k t / L}, \quad (3)$$

where k is the frequency index. The resulting frequency features are concatenated with the input time series, resulting in a tensor of shape $\mathbb{R}^{B \times L \times D \times 2}$.

2. Periodicity Encoding: Temporal dependencies are encoded using sine and cosine functions for each time step:

$$\text{encoding}(t) = \left[\sin\left(\frac{2\pi t}{P}\right), \cos\left(\frac{2\pi t}{P}\right) \right], \quad (4)$$

where P is the periodicity hyperparameter. These encodings are concatenated with the input time series, resulting in a tensor of shape $\mathbb{R}^{B \times L \times D \times 3}$. Complete periodic parameter settings can be found in [Appendix A](#).

Multi-scale Convolution: The concat tensor is processed through multiple convolutional layers to extract hierarchical temporal patterns. A 1D convolutional layer captures local dependencies, transforming the input into $\mathbb{R}^{B \times D \times H_{\text{hidden}} \times L}$, where H_{hidden} is the hidden dimension. Averaging along D yields $\mathbb{R}^{B \times H_{\text{hidden}} \times L}$. Two 2D convolutional layers follow: the first halves the channel dimension, and the second maps features to C output channels, producing the final output capturing both local and global temporal structures.

Image Interpolation & Normalization: The output tensor is resized to the desired image dimensions (H, W) using bilinear interpolation. For a target pixel (x, y) , the interpolated value $\mathbf{I}(x, y)$ is computed as follows:

$$\mathbf{I}(x, y) = \sum_{i=1}^2 \sum_{j=1}^2 \mathbf{I}(x_i, y_j) \cdot w_{ij}, \quad (5)$$

$$\text{Inorm} = 255 \cdot \frac{\mathbf{I}_{\text{raw}} - \text{Min}(\mathbf{I}_{\text{raw}})}{\text{Max}(\mathbf{I}_{\text{raw}}) - \text{Min}(\mathbf{I}_{\text{raw}}) + \epsilon}, \quad (6)$$

where (x_i, y_j) are the coordinates of the four nearest neighbors, w_{ij} are weights based on relative distances, and $\epsilon = 10^{-5}$ prevents division by zero. Pixel values are scaled to $[0, 255]$ via min-max normalization, producing the normalized image $\mathbf{I}_{\text{norm}} \in \mathbb{R}^{B \times C \times H \times W}$ (C is the number of channels). This ensures alignment with the VLM vision encoder's input distribution for effective feature extraction. Example images and descriptions can see [Appendix C](#).

3.3. Text-Augmented Learner (TAL)

The TAL module provides contextual textual representations, either pre-defined (e.g., expert annotations) or dynamically generated, offering flexibility across diverse scenarios.

For dynamically generated prompts, TAL extracts key statistical properties from the input time series, including:

- Range: minimum and maximum values,
- Central tendency: median value,
- Trend: upward/downward based on first-order differences,
- Periodicity: dominant frequency components,
- Task context: forecasting horizon and historical window,
- Dataset characteristics: domain-specific descriptions.

These features are formatted into structured textual prompts. For example, the generated prompt might take the form:

“This is a time series transformed image highlighting its trends, periodic and change patterns. Dataset: {description}. Task: Forecast the next {pred_len} steps using the past {seq_len} steps. Input statistics: min value = {min_val}, max value = {max_val}, median value = {median_val}, the overall trend is {trend_direction}.”

When domain-specific knowledge is available (e.g., in medical diagnostics or financial analysis), TAL incorporates pre-defined textual descriptions. These are combined with dynamically generated prompts to enhance contextual understanding. The final textual representations are processed by the VLM text encoder, producing contextual embeddings that complement visual and temporal features.

By supporting both pre-defined and dynamically generated textual representations, TAL provides a flexible and adaptive mechanism for leveraging textual information in time series forecasting. This adaptability ensures that the model can effectively handle diverse scenarios, from general-purpose forecasting to domain-specific applications.

3.4. Multimodal Fusion with VLMs

The multimodal fusion pipeline integrates visual (VAL), textual (TAL), and temporal (RAL) information, leverag-

ing their complementary strengths to enhance time series forecasting. It consists of three key steps:

Multimodal Embeddings Extraction: The generated images and text are processed by a frozen VLM (e.g., ViLT or CLIP), producing multimodal embeddings of shape $\mathbb{R}^{B \times L_f \times d_h}$, where B is the batch size, L_f is the sequence length, and d_h is the VLM's hidden dimension. These embeddings capture visual and textual context, leveraging the VLM's pre-trained multimodal understanding capabilities.

Temporal Feature Fusion: To address the distribution shift between temporal and multimodal features, both modalities are projected into a shared d_{model} -dimensional space. Temporal memory embeddings \mathbf{F}_{tem} from RAL encode high-level temporal patterns and serve as queries in a cross-modal multi-head attention (CM-MHA) mechanism, while the multimodal embeddings \mathbf{F}_{mm} from the VLM serve as keys and values. The CM-MHA is defined as:

$$\text{CM-MHA}(Q, K, V) = \text{Cat}(\text{head}_1, \dots, \text{head}_h)W^O, \quad (7)$$

$$\text{head}_i = \text{softmax} \left(\frac{QW_i^Q (KW_i^K)^\top}{\sqrt{d_k}} \right) VW_i^V. \quad (8)$$

where $Q = \mathbf{F}_{\text{tem}}W^Q$, $K = \mathbf{F}_{\text{mm}}W^K$, and $V = \mathbf{F}_{\text{mm}}W^V$. Here, W_i^Q , W_i^K , W_i^V , and W^O are learnable projection matrices. $d_k = d_{\text{model}}/h$ is the head dimension, and h is the number of attention heads. This mechanism aligns and integrates temporal and multimodal features, capturing both fine-grained patterns and high-level context. A residual connection and layer normalization stabilize training:

$$\mathbf{F}_{\text{attn}} = \text{LayerNorm}(\mathbf{F}_{\text{tem}} + \text{CM-MHA}(Q, K, V)). \quad (9)$$

A gated fusion mechanism further enhances the output by dynamically weighting each modality:

$$\mathbf{G} = \sigma(\mathbf{W}_g[\mathbf{F}_{\text{tem}}; \mathbf{F}_{\text{mm}}] + \mathbf{b}_g), \quad (10)$$

$$\mathbf{F}_{\text{fused}} = \mathbf{G} \odot \mathbf{F}_{\text{attn}} + (1 - \mathbf{G}) \odot \mathbf{F}_{\text{mm}}, \quad (11)$$

where \mathbf{W}_g and \mathbf{b}_g are learnable parameters, and $\sigma(\cdot)$ is the sigmoid function. This gated mechanism adaptively balances temporal and multimodal features for robust fusion.

Forecasting: The fused embedding is processed by a fine-tuned predictor, consisting of fully connected layers, to generate forecasts $\hat{y} \in \mathbb{R}^{B \times T_{\text{pred}} \times D}$. By combining visual, textual, and temporal modalities, the pipeline captures both detailed patterns and high-level context, leveraging pre-trained VLMs for enhanced forecasting across diverse scenes.

3.5. Optimization

The model is trained end-to-end using a mean squared error (MSE) loss to optimize forecasting performance. Given

historical observations $\mathbf{X} \in \mathbb{R}^{N \times T}$ (with N variables and T time steps), the goal is to predict future values $\hat{\mathbf{Y}} \in \mathbb{R}^{N \times H}$ for H time steps. The optimization objective is:

$$\mathcal{L} = \frac{1}{H} \sum_{h=1}^H \|\hat{\mathbf{Y}}_h - \mathbf{Y}_h\|^2, \quad (12)$$

where $\hat{\mathbf{Y}}_h$ and \mathbf{Y}_h are predicted and ground truth values at time step h . The pre-trained VLM is frozen, and only lightweight components are optimized:

- **RAL:** Patch embedding layer, memory queries, and attention mechanisms - capture temporal dependencies.
- **VAL:** Multi-scale convolutional layers, frequency encoding, and periodicity encoding modules - transform time series into informative images.
- **Multimodal Fusion:** Gating network, projection layers, and multi-head cross-attention - balance modality contributions (temporal, visual, and textual).
- **Predictor:** fully connected layers - maps fused embeddings to forecasts.

This strategy adapts the VLM to time series forecasting, achieving robust performance with minimal overhead.

4. Experiments

Datasets and Metrics. We evaluate Time-VLM on seven widely-used time series datasets spanning diverse domains, including energy consumption (ETTh1, ETTh2, ETTm1, ETTm2), weather forecasting, electricity load prediction (ECL, 321 variables), and traffic flow estimation (Traffic, 862 variables) (Zhou et al., 2021; Lai et al., 2018). These datasets, extensively adopted for benchmarking long-term forecasting models (Wu et al., 2023a), exhibit varying characteristics in sampling frequency, dimensionality, and temporal patterns. For short-term forecasting, we utilize the M4 benchmark (Makridakis et al., 2018), which encompasses marketing data at various sampling frequencies. Forecasting performance is evaluated using Mean Absolute Error (MAE) and Mean Squared Error (MSE), following standard practices in the field. Additional details on datasets and metrics are provided in Appendix A.1 and A.3.

Baselines. We compare Time-VLM with state-of-the-art time series models, including text-augmented methods like TimeLLM (2024), GPT4TS (2023), and LLMTTime (2023); vision-augmented methods like TimesNet (2023b); traditional deep models like PatchTST (2023), ESTformer (2022), Non-Stationary Transformer (2022b), FEDformer (2022), Autoformer (2021), Informer (2021), and Reformer (2020); and recent competitive models like DLinear (2023), LightTS (2022), N-HiTS (2023), and N-BEATS (2020). Notably, Time-VLM is the first framework combining three modalities for time series forecasting. Performance results for some baselines are cited from (2024a) where applicable.

Table 1: Few-shot learning on 5% training data. Results are averaged over forecasting horizons $H \in \{96, 192, 336, 720\}$. Lower values indicate better performance. Full results see Section B.1. **Red**: best, **Blue**: second best.

Methods	Time-VLM _{143M} (Ours)	Time-LLM _{3405M} (2024)	GPT4TS (2023)	DLinear (2023)	PatchTST (2023)	TimesNet (2023a)	FEDformer (2022)	Autoformer (2021)	Stationary (2022b)	ETSformer (2022)	LightTS (2022)	Informer (2021)	Reformer (2020)	
Metric	MSE	MAE	MSE	MAE	MSE	MAE	MSE	MAE	MSE	MAE	MSE	MAE	MSE	MAE
<i>ETTh1</i>	0.442	0.453	0.627	0.543	0.681	0.560	0.750	0.611	0.694	0.569	0.925	0.647	0.658	0.562
<i>ETTh2</i>	0.354	0.402	0.382	0.418	0.400	0.433	0.694	0.577	0.827	0.615	0.439	0.448	0.463	0.454
<i>ETTm1</i>	0.364	0.385	0.425	0.434	0.472	0.450	0.400	0.417	0.526	0.476	0.717	0.561	0.730	0.592
<i>ETTm2</i>	0.262	0.323	0.274	0.323	0.308	0.346	0.399	0.426	0.314	0.352	0.344	0.372	0.381	0.404
<i>Weather</i>	0.240	0.280	0.260	0.309	0.263	0.301	0.263	0.308	0.269	0.303	0.298	0.318	0.309	0.353
<i>ECL</i>	0.218	0.315	0.179	0.268	0.178	0.273	0.176	0.275	0.181	0.277	0.402	0.453	0.266	0.353
<i>Traffic</i>	0.558	0.410	0.423	0.298	0.434	0.305	0.450	0.317	0.418	0.296	0.867	0.493	0.676	0.423

Table 2: Few-shot learning on 10% training data. We use the same protocol in Table 1. Full results see Section B.1.

Methods	Time-VLM _{143M} (Ours)	Time-LLM _{3405M} (2024)	GPT4TS (2023)	DLinear (2023)	PatchTST (2023)	TimesNet (2023a)	FEDformer (2022)	Autoformer (2021)	Stationary (2022b)	ETSformer (2022)	LightTS (2022)	Informer (2021)	Reformer (2020)	
Metric	MSE	MAE	MSE	MAE	MSE	MAE	MSE	MAE	MSE	MAE	MSE	MAE	MSE	MAE
<i>ETTh1</i>	0.431	0.442	0.556	0.522	0.590	0.525	0.691	0.600	0.633	0.542	0.869	0.628	0.639	0.561
<i>ETTh2</i>	0.361	0.405	0.370	0.394	0.397	0.421	0.605	0.538	0.415	0.431	0.479	0.465	0.460	0.475
<i>ETTm1</i>	0.360	0.382	0.404	0.427	0.464	0.441	0.411	0.429	0.501	0.466	0.677	0.537	0.722	0.605
<i>ETTm2</i>	0.263	0.323	0.277	0.323	0.293	0.335	0.316	0.368	0.296	0.343	0.320	0.353	0.463	0.488
<i>Weather</i>	0.233	0.274	0.234	0.273	0.238	0.275	0.241	0.283	0.242	0.279	0.279	0.301	0.284	0.324
<i>ECL</i>	0.198	0.291	0.175	0.270	0.176	0.269	0.180	0.280	0.180	0.273	0.323	0.392	0.346	0.427
<i>Traffic</i>	0.484	0.357	0.429	0.306	0.440	0.310	0.447	0.313	0.430	0.305	0.951	0.535	0.663	0.425

Table 3: Zero-shot learning results. Full results see Section B.2.

Methods	Time-VLM _{143M} (Ours)	Time-LLM _{3405M} (2024)	LLMTime (2023)	GPT4TS (2023)	DLinear (2023)	PatchTST (2023)		
Metric	MSE	MAE	MSE	MAE	MSE	MAE	MSE	MAE
<i>ETTh1</i> \rightarrow <i>ETTh2</i>	0.338	0.385	0.353	0.387	0.992	0.708	0.400	0.422
<i>ETTh1</i> \rightarrow <i>ETTm2</i>	0.293	0.350	0.273	0.340	1.867	0.869	0.325	0.363
<i>ETTh2</i> \rightarrow <i>ETTh1</i>	0.496	0.480	0.479	0.474	1.961	0.981	0.757	0.578
<i>ETTh2</i> \rightarrow <i>ETTm2</i>	0.297	0.353	0.272	0.341	1.867	0.869	0.335	0.370
<i>ETTm1</i> \rightarrow <i>ETTh2</i>	0.354	0.397	0.381	0.412	0.992	0.708	0.433	0.439
<i>ETTm1</i> \rightarrow <i>ETTm2</i>	0.264	0.319	0.268	0.320	1.867	0.869	0.313	0.348
<i>ETTm2</i> \rightarrow <i>ETTh2</i>	0.359	0.399	0.354	0.400	0.992	0.708	0.435	0.443
<i>ETTm2</i> \rightarrow <i>ETTm1</i>	0.432	0.426	0.414	0.438	1.933	0.984	0.769	0.567

Implementation Details. We compare Time-VLM against state-of-the-art models using a unified evaluation pipeline, following the configurations in (Wu et al., 2023a) for fair comparison. ViLT (Kim et al., 2021) is the default backbone, with "vilt-b32-finetuned-coco". Other VLMs like CLIP and BLIP-2 are also supported. All models are trained with the Adam optimizer (learning rate 10^{-3} , halved every epoch), a batch size of 32, and a maximum of 10 epochs with early stopping. Experiments are conducted on an Nvidia RTX A6000 GPU with 48GB memory. Additional optimization details are in Appendix A.2.

4.1. Few-shot Forecasting

We evaluate the few-shot capabilities of Time-VLM by testing its performance using only 5% or 10% of training data. This assesses its ability to combine pre-trained multimodal knowledge from VLM with time series-specific features for effective forecasting under minimal task-specific data.

As shown in Table 1 and Table 2, Time-VLM consistently outperforms most baselines across datasets. For example,

on ETTh1 with 5% training data, Time-VLM reduces MSE by 29.5% and MAE by 16.6% compared to the second-best model, TimeLLM. On ETTm1 with 10% data, it surpasses TimeLLM by 11.1% in MSE and 10.5% in MAE. On Weather with 5% data, Time-VLM outperforms TimeLLM by 7.7% in MSE and 9.4% in MAE.

The performance gap between Time-VLM and traditional models (e.g., PatchTST, FEDformer) is more pronounced in few-shot settings, demonstrating the superiority of multimodality in data-scarce scenarios. Notably, Time-VLM achieves this with only 143M parameters, significantly fewer than TimeLLM's 3405M, highlighting its efficiency.

4.2. Zero-shot Forecasting

We evaluate the zero-shot capability of Time-VLM in cross-domain settings, where the model predicts on unseen datasets by effectively leveraging knowledge from unrelated domains. To ensure a more comprehensive and rigorous comparison, we use the ETT datasets as Time-LLM (Jin et al., 2024), with results summarized in Table 3.

Time-VLM demonstrates strong zero-shot generalization, consistently outperforming or matching state-of-the-art baselines with fewer parameters. For example, in *ETTh1* \rightarrow *ETTh2*, Time-VLM surpasses TimeLLM with a 4.2% lower MSE and 0.5% lower MAE. In *ETTm1* \rightarrow *ETTh2*, it outperforms TimeLLM by 7.1% in MSE and 3.6% in MAE. In *ETTm2* \rightarrow *ETTh2*, Time-VLM achieves competitive performance, closely matching TimeLLM with only a 1.4% difference in MSE and 0.3% in MAE.

Table 4: Short-term time series forecasting results on M4. The forecasting horizons are in [6, 48] and the three rows provided are weighted averaged from all datasets under different sampling intervals. Full results see Section B.3.

Methods	Time-VLM _{143M} (Ours)	Time-LLM _{3405M} (2024)	GPT4TS (2023)	TimesNet (2023a)	PatchTST (2023)	N-HiTS (2023)	N-BEATS (2020)	ETSformer (2022)	LightTS (2022)	DLinear (2023)	FEDformer (2022)	Stationary (2022b)	Autoformer (2021)	Informer (2021)	Reformer (2020)	
Average	SMAPE	11.894	11.983	12.690	12.880	12.059	12.035	12.250	14.718	13.525	13.639	13.160	12.780	12.909	14.086	18.200
	MASE	1.592	1.595	1.808	1.836	1.623	1.625	1.698	2.408	2.111	2.095	1.775	1.756	1.771	2.718	4.223
	OWA	0.855	0.859	0.940	0.955	0.869	0.869	0.896	1.172	1.051	1.051	0.949	0.930	0.939	1.230	1.775

Table 5: Long-term forecasting results. We use the same protocol in Table 1. Full results see in Section B.4.

Methods	Time-VLM _{143M} (Ours)	Time-LLM _{3405M} (2024)	GPT4TS (2023)	DLinear (2023)	PatchTST (2023)	TimesNet (2023a)	FEDformer (2022)	Autoformer (2021)	Stationary (2022b)	ETSformer (2022)	LightTS (2022)	Informer (2021)	Reformer (2020)													
Metric	MSE	MAE	MSE	MAE	MSE	MAE	MSE	MAE	MSE	MAE	MSE	MAE	MSE	MAE	MSE	MAE										
ETTh1	0.405	0.420	0.408	0.423	0.465	0.455	0.422	0.437	0.413	0.430	0.458	0.450	0.440	0.460	0.496	0.487	0.570	0.537	0.542	0.510	0.491	0.479	0.1040	0.795	0.1029	0.805
ETTh2	0.341	0.391	0.334	0.383	0.381	0.412	0.431	0.446	0.330	0.379	0.414	0.427	0.437	0.449	0.450	0.459	0.526	0.516	0.439	0.452	0.602	0.543	0.431	1.729	6.736	2.191
ETTm1	0.347	0.377	0.329	0.372	0.388	0.403	0.357	0.378	0.351	0.380	0.400	0.406	0.448	0.452	0.588	0.517	0.481	0.456	0.429	0.425	0.435	0.437	0.961	0.734	0.799	0.671
ETTm2	0.248	0.311	0.251	0.313	0.284	0.339	0.267	0.333	0.255	0.315	0.291	0.333	0.305	0.349	0.327	0.371	0.306	0.347	0.293	0.342	0.409	0.436	1.410	0.810	1.479	0.915
Weather	0.224	0.263	0.225	0.257	0.237	0.270	0.248	0.300	0.225	0.264	0.259	0.287	0.309	0.360	0.338	0.382	0.288	0.314	0.271	0.334	0.261	0.312	0.634	0.548	0.803	0.656
Electricity	0.172	0.273	0.158	0.252	0.167	0.263	0.166	0.263	0.161	0.252	0.192	0.295	0.214	0.327	0.227	0.338	0.193	0.296	0.208	0.323	0.229	0.329	0.311	0.397	0.338	0.422
Traffic	0.419	0.303	0.388	0.264	0.414	0.294	0.433	0.295	0.390	0.263	0.620	0.336	0.610	0.376	0.628	0.379	0.624	0.340	0.621	0.396	0.622	0.392	0.764	0.416	0.741	0.422

4.3. Short-term Forecasting

For short-term forecasting, we evaluate Time-VLM on the M4 benchmark, which includes marketing data at various sampling frequencies. Performance is measured using SMAPE, MASE, and OWA metrics, averaged across datasets and sampling intervals (see Table 4).

Time-VLM demonstrates strong performance, consistently outperforming state-of-the-art baselines across all metrics. For instance, it surpasses the second-best model, Time-LLM, with improvements of 0.7% in SMAPE, 0.2% in MASE, and 0.5% in OWA, all while utilizing significantly fewer parameters and computational resources. Compared to traditional models like PatchTST and N-HiTS, the performance gains more, highlighting the benefit of multimodal knowledge in short-term forecasting. These gains stem from Time-VLM’s integration of temporal, visual, and textual data, capturing richer features for improved accuracy.

4.4. Long-term Forecasting

We evaluate the long-term forecasting capabilities of Time-VLM across diverse temporal horizons and datasets.

As shown in Table 5, Time-VLM achieves competitive performance compared to state-of-the-art baselines. For example, on ETTh1, Time-VLM surpasses TimeLLM with 0.7% improvements in MSE and MAE. On ETTh2, it outperforms TimeLLM by 1.2% in MSE and 0.6% in MAE. However, on Weather, Time-VLM slightly trails TimeLLM with a 0.4% higher MSE and 2.3% higher MAE.

Overall, Time-VLM demonstrates robust performance across diverse tasks and datasets, highlighting its generalization and efficiency. By leveraging multimodal knowledge, it consistently outperforms state-of-the-art baselines with significantly fewer parameters (143M vs. TimeLLM’s 3405M), making it a practical solution for real-world applications.

4.5. Model Analysis

Ablation Studies: Table 6 evaluates the contributions of key components of Time-VLM, including the RAL, VAL, and TAL. Results are averaged across forecasting horizons $H \in \{96, 192, 336, 720\}$ on the Weather dataset, with performance degradation (%Deg) measured for each variant.

Table 6: Ablation study on multimodal components.

Horizon	Full		w/o RAL		w/o VAL		w/o TAL	
	MSE	MAE	MSE	MAE	MSE	MAE	MSE	MAE
96	0.160	0.213	0.273	0.324	0.213	0.266	0.165	0.218
192	0.203	0.252	0.297	0.338	0.237	0.298	0.208	0.257
336	0.253	0.291	0.325	0.354	0.255	0.302	0.258	0.295
720	0.317	0.340	0.369	0.383	0.309	0.357	0.322	0.345
Avg	0.233	0.274	0.316	0.350	0.254	0.306	0.238	0.279
%Deg	—	—	35.6% \uparrow	27.7% \uparrow	9.0% \uparrow	11.7% \uparrow	2.1% \uparrow	1.8% \uparrow

The study highlights the critical role of each component. Removing the RAL causes the largest performance drop (35.6% in MSE and 27.7% in MAE), emphasizing its importance in capturing temporal dependencies through memory bank interactions. The VAL, which transforms time series into visual representations, is essential, with its exclusion leading to significant degradation (9.0% in MSE and 11.7% in MAE). This underscores its ability to preserve fine-grained temporal patterns using VLM vision encoder. In contrast, removing the TAL results in minor degradation (2.1% in MSE and 1.8% in MAE), likely due to sparse textual tokens in the VLM output (e.g., 11 out of 156 in ViLT). While the TAL provides valuable semantic context, its impact is limited by the VLM’s temporal understanding. Future work could explore larger VLMs with extended textual inputs to enhance temporal-semantic alignment.

Multimodal and Few/Zero-shot Analysis: Time-VLM’s few-shot and zero-shot capabilities arise from its integration of temporal, visual, and textual modalities. The RAL models temporal dependencies through memory bank interactions, ensuring robust feature extraction with limited

data. The VAL captures visually interpretable features (e.g., trend, seasonality, periodicity) in domain-agnostic visual representations, while the TAL generates contextual descriptions, providing semantic insights for better generalization. Together, these components enable Time-VLM to leverage pre-trained multimodal knowledge, making it highly adaptable to new tasks and domains with minimal training data.

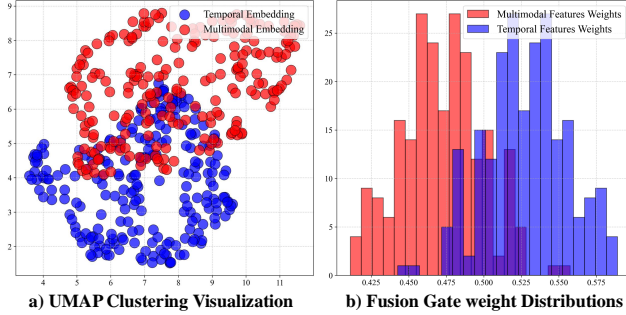


Figure 3: 2D UMAP visualization (Left) and Gate weight distributions (Right) of multimodal and temporal memory embeddings, highlighting their complementary behavior.

To validate the adaptation of VLM capabilities to time series, we analyze the similarity between RAL (temporal) and TAL/VAL (multimodal) embeddings. Figure 3 visualizes their complementary behavior. The left panel shows balanced gate weight distributions, indicating effective fusion of multimodal and temporal representations. The right panel’s UMAP visualization reveals distinct yet overlapping clusters, confirming successful integration of multimodal information while preserving unique characteristics. This demonstrates Time-VLM’s ability to adapt VLM-derived embeddings for robust time series analysis.

Computation Studies: Time-VLM demonstrates strong computational efficiency, as shown in Table 7. With only 143.6M parameters (1/20 of Time-LLM’s 3404.6M), memory usage scales from 1968 MiB (Weather) to 24916 MiB (Traffic), adapting to dataset complexity. Inference speed ranges from 0.2057s/iter (ECL) to 0.4809s/iter (ETTh1), efficiently handling varying loads. In contrast, Time-LLM requires over 37GB of memory even for smaller datasets like ETTh1 and ETTh2, making it infeasible for larger datasets such as Weather, ECL, and Traffic. This highlights Time-VLM’s lightweight design and practical scalability.

Table 7: Computational efficiency comparison between Time-VLM and Time-LLM across datasets. “-” denotes memory exceeds 49GB, infeasible on a single GPU. Results are averaged over multiple prediction steps under consistent conditions.

Method	Metric	ETTh1	ETTh2	ETTm1	ETTm2	Weather	ECL	Traffic
Time-VLM	Param. (M)	143.6	143.6	143.6	143.6	143.6	143.6	143.6
	Mem. (MiB)	2630	2630	2640	2640	1968	10818	24916
	Speed (s/iter)	0.481	0.438	0.277	0.210	0.296	0.206	0.323
Time-LLM	Param. (M)	3404.6	3404.6	3404.6	3404.6	-	-	-
	Mem. (MiB)	37723	37723	37849	37849	-	-	-
	Speed (s/iter)	0.607	0.553	0.349	0.265	-	-	-

Hyperparameter Studies: We analyze key hyperparameters’ impact on performance, as shown in Figure 4. The sequence length performs best between 96 and 1024 timesteps, with 512 being optimal for most datasets. Longer sequences introduce noise without significant gains. The normalization constant peaks at 0.4, while the model dimension performs best at 128 for simpler datasets (e.g., ETTh1, ETTh2) and larger values for complex ones (e.g., Traffic, Weather). The gate network dimension, controlling multimodal fusion, achieves optimal results at 256 across most datasets.

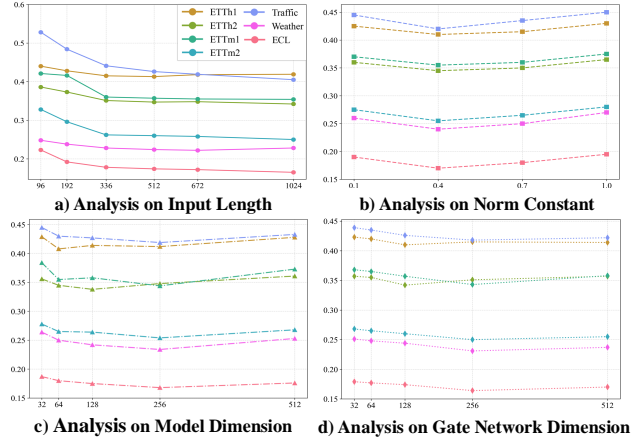


Figure 4: Hyperparameters sensitivity analysis on input length, normalization constant, dimension of model and dimension of gate network, reflected by MAE.

5. Conclusion

We presented Time-VLM, a novel framework leveraging pretrained VLMs to unify temporal, visual, and textual modalities for time series forecasting. By integrating the RAL, VAL, and TAL, Time-VLM bridges modality gaps, enabling rich cross-modal interactions. Extensive experiments demonstrate state-of-the-art performance across various datasets, especially in few-shot and zero-shot scenarios, outperforming existing methods while maintaining efficiency. Our work establishes a new direction for multimodal time series forecasting, highlighting the potential of VLMs in capturing temporal dynamics and semantic context.

Notably, Time-VLM operates can solely on original time series data without external information, ensuring fair comparisons and showcasing its ability to generate textual and visual representations directly from the data for self-augmentation. This design not only enhances accuracy but also emphasizing the framework’s robustness, particularly in domains where external data is scarce or unavailable.

Future work may explore adaptive visual transformations for complex patterns, enhancing text utilization, extending to multi-task, and developing more efficient multimodal time series foundation models. For details, see Appendix D.

Impact Statement

This paper presents work whose goal is to advance the field of Machine Learning by integrating temporal, visual, and textual modalities for time series forecasting. While our approach improves accuracy and cross-domain generalization, we acknowledge potential risks such as data privacy concerns, algorithmic bias, and increased computational costs. We encourage further research into mitigating these risks to ensure responsible deployment in high-stakes applications.

References

Challu, C., Olivares, K. G., Oreshkin, B. N., Ramirez, F. G., Canseco, M. M., and Dubrawski, A. Nhits: neural hierarchical interpolation for time series forecasting. In *Proceedings of the AAAI Conference on Artificial Intelligence*, volume 37, pp. 6989–6997, 2023.

Chang, C., Peng, W.-C., and Chen, T.-F. Llm4ts: Two-stage fine-tuning for time-series forecasting with pre-trained llms. *arXiv preprint arXiv:2308.08469*, 2023.

Chen, M., Shen, L., Li, Z., Wang, X. J., Sun, J., and Liu, C. Visions: Visual masked autoencoders are free-lunch zero-shot time series forecasters, 2024. URL <https://arxiv.org/abs/2408.17253>.

Deb, C., Zhang, F., Yang, J., Lee, S. E., and Shah, K. W. A review on time series forecasting techniques for building energy consumption. *Renewable and Sustainable Energy Reviews*, 74:902–924, 2017.

Gruver, N., Finzi, M., Qiu, S., and Wilson, A. G. Large language models are zero-shot time series forecasters. In *Advances in Neural Information Processing Systems*, 2023.

Idrees, S. M., Alam, M. A., and Agarwal, P. A prediction approach for stock market volatility based on time series data. *IEEE Access*, 7:17287–17298, 2019.

Jia, C., Yang, Y., Xia, Y., Chen, Y.-T., Parekh, Z., Pham, H., Le, Q., Sung, Y.-H., Li, Z., and Duerig, T. Scaling up visual and vision-language representation learning with noisy text supervision. In *International conference on machine learning*, pp. 4904–4916. PMLR, 2021.

Jin, M., Wang, S., Ma, L., Chu, Z., Zhang, J. Y., Shi, X., Chen, P.-Y., Liang, Y., Li, Y.-F., Pan, S., and Wen, Q. Time-LLM: Time series forecasting by reprogramming large language models. In *International Conference on Learning Representations (ICLR)*, 2024.

Karevan, Z. and Suykens, J. A. Transductive lstm for time-series prediction: An application to weather forecasting. *Neural Networks*, 125:1–9, 2020.

Kim, W., Son, B., and Kim, I. Vilt: Vision-and-language transformer without convolution or region supervision. In *International conference on machine learning*, pp. 5583–5594. PMLR, 2021.

Kitaev, N., Kaiser, Ł., and Levskaya, A. Reformer: The efficient transformer. In *International Conference on Learning Representations*, 2020.

Lai, G., Chang, W.-C., Yang, Y., and Liu, H. Modeling long-and short-term temporal patterns with deep neural networks. In *The 41st international ACM SIGIR conference on research & development in information retrieval*, pp. 95–104, 2018.

Li, J., Li, D., Savarese, S., et al. Blip-2: Bootstrapping language-image pre-training with frozen image encoders and large language models. In *International conference on machine learning*, pp. 19730–19742. PMLR, 2023.

Li, S., Jin, X., Xuan, Y., Zhou, X., Chen, W., Wang, Y.-X., and Yan, X. Enhancing the locality and breaking the memory bottleneck of transformer on time series forecasting. In *Advances in neural information processing systems*, 2019.

Li, X., Kang, Y., and Li, F. Forecasting with time series imaging. *Expert Systems with Applications*, 160:113680, 2020.

Liang, Y., Wen, H., Nie, Y., Jiang, Y., Jin, M., Song, D., Pan, S., and Wen, Q. Foundation models for time series analysis: A tutorial and survey. In *Proceedings of the 30th ACM SIGKDD conference on knowledge discovery and data mining*, pp. 6555–6565, 2024.

Liu, H., Li, C., Wu, Q., and Lee, Y. J. Visual instruction tuning. *arXiv preprint arXiv:2304.08485*, 2023.

Liu, Q., Liu, X., Liu, C., Wen, Q., and Liang, Y. Time-ffm: Towards lm-empowered federated foundation model for time series forecasting. *arXiv preprint arXiv:2405.14252*, 2024a.

Liu, S., Yu, H., Liao, C., Li, J., Lin, W., Liu, A. X., and Dustdar, S. Pyraformer: Low-complexity pyramidal attention for long-range time series modeling and forecasting. In *International Conference on Learning Representations*, 2022a.

Liu, X., Hu, J., Li, Y., Diao, S., Liang, Y., Hooi, B., and Zimmermann, R. Unitime: A language-empowered unified model for cross-domain time series forecasting. In *Proceedings of the ACM on Web Conference 2024*, pp. 4095–4106, 2024b.

Liu, Y., Wu, H., Wang, J., and Long, M. Non-stationary transformers: Exploring the stationarity in time series

forecasting. *Advances in Neural Information Processing Systems*, 35:9881–9893, 2022b.

Makridakis, S., Spiliotis, E., and Assimakopoulos, V. The m4 competition: Results, findings, conclusion and way forward. *International Journal of Forecasting*, 34(4): 802–808, 2018.

Medsker, L. R., Jain, L., et al. Recurrent neural networks. *Design and Applications*, 5(64-67):2, 2001.

Nie, Y., Nguyen, N. H., Sinthong, P., and Kalagnanam, J. A time series is worth 64 words: Long-term forecasting with transformers. In *International Conference on Learning Representations*, 2023.

Oreshkin, B. N., Carpov, D., Chapados, N., and Bengio, Y. N-beats: Neural basis expansion analysis for interpretable time series forecasting. In *International Conference on Learning Representations*, 2020.

Radford, A., Kim, J. W., Hallacy, C., Ramesh, A., Goh, G., Agarwal, S., Sastry, G., Askell, A., Mishkin, P., Clark, J., et al. Learning transferable visual models from natural language supervision. In *International conference on machine learning*, pp. 8748–8763. PMLR, 2021.

Sood, S., Zeng, Z., Cohen, N., Balch, T., and Veloso, M. Visual time series forecasting: an image-driven approach. In *Proceedings of the Second ACM International Conference on AI in Finance*, pp. 1–9, 2021.

Wang, S., Li, J., Shi, X., Ye, Z., Mo, B., Lin, W., Ju, S., Chu, Z., and Jin, M. Timemixer++: A general time series pattern machine for universal predictive analysis. *arXiv preprint arXiv:2410.16032*, 2024.

Woo, G., Liu, C., Sahoo, D., Kumar, A., and Hoi, S. Ets-former: Exponential smoothing transformers for time-series forecasting. In *arXiv preprint arXiv:2202.01381*, 2022.

Wu, H., Xu, J., Wang, J., and Long, M. Autoformer: Decomposition transformers with auto-correlation for long-term series forecasting. *Advances in Neural Information Processing Systems*, 34:22419–22430, 2021.

Wu, H., Hu, T., Liu, Y., Zhou, H., Wang, J., and Long, M. Timesnet: Temporal 2d-variation modeling for general time series analysis. In *International Conference on Learning Representations*, 2023a.

Wu, H., Hu, T., Liu, Y., Zhou, H., Wang, J., and Long, M. Timesnet: Temporal 2d-variation modeling for general time series analysis. In *International Conference on Learning Representations*, 2023b.

Zeng, A., Chen, M., Zhang, L., and Xu, Q. Are transformers effective for time series forecasting? In *Proceedings of the AAAI conference on artificial intelligence*, volume 37, pp. 11121–11128, 2023.

Zhang, T., Zhang, Y., Cao, W., Bian, J., Yi, X., Zheng, S., and Li, J. Less is more: Fast multivariate time series forecasting with light sampling-oriented mlp structures. *arXiv preprint arXiv:2207.01186*, 2022.

Zheng, J. and Huang, M. Traffic flow forecast through time series analysis based on deep learning. *IEEE Access*, 8: 82562–82570, 2020.

Zhou, H., Zhang, S., Peng, J., Zhang, S., Li, J., Xiong, H., and Zhang, W. Informer: Beyond efficient transformer for long sequence time-series forecasting. In *Proceedings of the AAAI conference on Artificial Intelligence*, pp. 11106–11115, 2021.

Zhou, T., Ma, Z., Wen, Q., Wang, X., Sun, L., and Jin, R. Fedformer: Frequency enhanced decomposed transformer for long-term series forecasting. In *International Conference on Machine Learning*, pp. 27268–27286, 2022.

Zhou, T., Niu, P., Wang, X., Sun, L., and Jin, R. One fits all: Power general time series analysis by pretrained lm. In *Advances in Neural Information Processing Systems*, 2023.

A. Experimental Details

A.1. Dataset Details

Table 8: Summary of benchmark datasets. Each dataset includes multiple time series (Dim.) with varying sequence lengths, split into training, validation, and testing sets. Data are collected at different frequencies across various domains.

Tasks	Dataset	Dim.	Series Length	Dataset Size	Frequency	Domain	Periodicity
Long-term Forecasting	ETTm1	7	{96, 192, 336, 720}	(34465, 11521, 11521)	15 min	Temperature	96
	ETTm2	7	{96, 192, 336, 720}	(34465, 11521, 11521)	15 min	Temperature	96
	ETTh1	7	{96, 192, 336, 720}	(8545, 2881, 2881)	1 hour	Temperature	24
	ETTh2	7	{96, 192, 336, 720}	(8545, 2881, 2881)	1 hour	Temperature	24
	Electricity	321	{96, 192, 336, 720}	(18317, 2633, 5261)	1 hour	Electricity	24
	Traffic	862	{96, 192, 336, 720}	(12185, 1757, 3509)	1 hour	Transportation	24
Short-term Forecasting	Weather	21	{96, 192, 336, 720}	(36792, 5271, 10540)	10 min	Weather	144
	M4 - Yearly	1	6	(23000, 0, 23000)	Yearly	Demographic	1
	M4 - Quarterly	1	8	(24000, 0, 24000)	Quarterly	Finance	4
	M4 - Monthly	1	18	(48000, 0, 48000)	Monthly	Industry	3
	M4 - Weekly	1	13	(359, 0, 359)	Weekly	Macro	4
	M4 - Daily	1	14	(4227, 0, 4227)	Daily	Micro	1
	M4 - Hourly	1	48	(414, 0, 414)	Hourly	Other	24

The benchmark datasets used in our experiments are summarized in Table 8. These datasets span diverse domains, including temperature monitoring (*ETTm1*, *ETTm2*, *ETTh1*, *ETTh2*), electricity consumption (*Electricity*), transportation (*Traffic*), and weather forecasting (*Weather*). Each dataset contains multiple time series with varying sequence lengths, split into training, validation, and testing sets. The datasets are collected at different frequencies, ranging from 15 minutes to yearly intervals, and exhibit distinct periodic patterns. For short-term forecasting, we utilize the M4 benchmark, which includes datasets with yearly, quarterly, monthly, weekly, daily, and hourly frequencies, covering domains such as finance, industry, and demographics. This diverse collection of datasets ensures a comprehensive evaluation of our method.

A.1.1. DATASET DESCRIPTION

The datasets used in our experiments are described below:

- **ECL:** Measurements of electric power consumption in one household with a one-minute sampling rate over 4 years. It includes various electrical quantities and sub-metering values, totaling 2,075,259 measurements from a house in Sceaux, France (December 2006 to November 2010).
- **ETT:** The Electricity Transformer Temperature (ETT) dataset, crucial for electric power deployment, contains 2 years of data from two counties in China. Subsets *ETTh1* and *ETTh2* provide 1-hour-level data, while *ETTm1* offers 15-minute-level data. Each point includes the target "oil temperature" and 6 power load features, with a 12/4/4 month train/val/test split.
- **Traffic:** Hourly data from the California Department of Transportation, describing road occupancy rates measured by sensors on San Francisco Bay area freeways.
- **Weather:** Recorded every 10 minutes throughout 2020, this dataset includes 21 meteorological indicators, such as air temperature and humidity.
- **M4:** A collection of 100,000 time series from the Makridakis Forecasting Competition, including yearly, quarterly, monthly, weekly, daily, and hourly data. The training sets have minimum observations of 13 (yearly), 16 (quarterly), 42 (monthly), 80 (weekly), 93 (daily), and 700 (hourly). Forecasts required are 6 (yearly), 8 (quarterly), 18 (monthly), 13 (weekly), 14 (daily), and 48 (hourly).

A.1.2. PERIODICITY PARAMETER

The *Periodicity* column in Table 8 specifies the periodicity hyperparameter P used in the periodicity encoding process. This parameter is derived from the inherent characteristics of each dataset and reflects the dominant temporal patterns, such as

daily, weekly, or seasonal cycles. For example, in the *ETTm1* and *ETTm2* datasets, which are sampled every 15 minutes, the periodicity $P = 96$ corresponds to a daily cycle (24 hours \times 4 samples per hour). Similarly, for the *ETTh1* and *ETTh2* datasets, sampled hourly, $P = 24$ represents a daily cycle. The *Weather* dataset, sampled every 10 minutes, has $P = 144$, reflecting a daily cycle (24 hours \times 6 samples per hour). For the M4 benchmark datasets, the periodicity values are set based on their sampling frequencies: $P = 1$ for yearly data, $P = 4$ for quarterly and weekly data, $P = 3$ for monthly data, and $P = 24$ for hourly data. These values are used in the periodicity encoding formula:

$$\text{encoding}(t) = \left[\sin\left(\frac{2\pi t}{P}\right), \cos\left(\frac{2\pi t}{P}\right) \right], \quad (13)$$

where t is the time step and P is the periodicity hyperparameter. The resulting encodings are concatenated with the input time series, enriching the model's ability to capture temporal dependencies and periodic patterns.

A.2. Optimization Settings

A.2.1. MODEL ARCHITECTURE PARAMETERS

Time-VLM consists of several key components, each with specific parameter configurations. Image representations are set to a size of 64×64 , balancing computational efficiency and temporal information preservation. The model backbone utilizes a hidden dimension of $d_{\text{model}} = 128$, while the encoder-decoder structure comprises $e_{\text{layers}} = 2$ encoder layers and $d_{\text{layers}} = 1$ decoder layer. A dropout rate of 0.1 is applied to mitigate overfitting during training. For efficient data loading, the model employs $\text{num_workers} = 32$ to parallelize data preprocessing tasks.

The gated fusion module is designed with a dimension of $d_{\text{fusion}} = 256$, facilitating the effective integration of multimodal features. The VLM component generates multimodal embeddings with a token length of $vlm_{\text{fused_len}} = 156$ and a hidden dimension of $vlm_{\text{hidden_dim}} = 768$, ensuring seamless compatibility with the pre-trained VLM's architecture.

Table 9: Default Model Architecture Parameters

Parameter	Default Value	Description
image_size	64	Size of generated image representation
d_model	128	Dimension of hidden embeddings
d_fusion	256	Dimension of gated fusion module
num_workers	32	Number of data loader workers
e_layers	2	Number of encoder layers
d_layers	1	Number of decoder layers
dropout	0.1	Dropout rate
vlm_fused_len	156	Token length of VLM multimodal embedding
vlm_hidden_dim	768	Hidden dimension of VLM

A.2.2. TRAINING PARAMETERS

We adopt a comprehensive training strategy with both general and task-specific parameters. The model is trained with a batch size of 32 and an initial learning rate of 0.001, using the *AdamW* optimizer. Early stopping with a patience of 3 epochs is implemented to prevent overfitting. The training process employs Mean Squared Error (MSE) as the primary loss function and runs for a maximum of 10 epochs. For time series processing, we use an input sequence length of 512 and prediction lengths of 96, 192, 336, or 720, depending on the task. The output dimension (c_{out}) varies by dataset: 7 for ETTh1/h2/m1/m2, 21 for Weather, 321 for Electricity, and 862 for Traffic. The periodicity parameter is set to 24 for ETTh1/h2, Electricity, and Traffic; 96 for ETTm1/m2; and 144 for Weather, ensuring alignment with dataset-specific temporal patterns. A normalization coefficient of 0.4 is applied to stabilize training dynamics. The patch embedding module uses a patch length of 16, a stride of 8, and padding of 8 to process the input sequences. The temporal memory mechanism employs 8 learnable queries and 4 attention heads to capture high-level dependencies. Additionally, the training process leverages automatic mixed precision (AMP) to accelerate training while maintaining numerical stability.

Table 10: Default Training Parameters

Parameter	Default Value	Description
batch_size	32	Training batch size
learning_rate	0.001	Initial learning rate
training_epochs	10	Number of training epochs
patience	3	Early stopping patience
loss	MSE	Mean square error
seq_len	512	Input sequence length
c_out	7 (ETTh1/h2/m1/m2) 21 (Weather) 321 (Electricity) 862 (Traffic)	Output dimension (dataset-specific)
pred_len	96/192/336/720	Prediction length
periodicity	24 (ETTh1/h2/Electricity/Traffic) 96 (ETTm1/m2) 144 (Weather)	Dataset periodicity (dataset-specific)
norm_const	0.4	Normalization coefficient
patch_len	16	Patch length
padding	8	Padding length
stride	8	Stride length
num_queries	8	Number of learnable queries for temporal memory
n_heads	4	Number of attention heads

A.3. Evaluation Metrics

For evaluation, we utilize mean squared error (MSE) and mean absolute error (MAE) for long-term forecasting. For short-term forecasting on the M4 benchmark, we adopt symmetric mean absolute percentage error (SMAPE), mean absolute scaled error (MASE), and overall weighted average (OWA), following the evaluation protocol of N-BEATS (Oreshkin et al., 2020). OWA is a specific metric used in the M4 competition. The metrics are calculated as follows:

$$\begin{aligned}
 \text{MSE} &= \frac{1}{H} \sum_{h=1}^T (\mathbf{Y}_h - \hat{\mathbf{Y}}_h)^2, & \text{MAE} &= \frac{1}{H} \sum_{h=1}^H |\mathbf{Y}_h - \hat{\mathbf{Y}}_h|, \\
 \text{SMAPE} &= \frac{200}{H} \sum_{h=1}^H \frac{|\mathbf{Y}_h - \hat{\mathbf{Y}}_h|}{|\mathbf{Y}_h| + |\hat{\mathbf{Y}}_h|}, & \text{MAPE} &= \frac{100}{H} \sum_{h=1}^H \frac{|\mathbf{Y}_h - \hat{\mathbf{Y}}_h|}{|\mathbf{Y}_h|}, \\
 \text{MASE} &= \frac{1}{H} \sum_{h=1}^H \frac{|\mathbf{Y}_h - \hat{\mathbf{Y}}_h|}{\frac{1}{H-s} \sum_{j=s+1}^H |\mathbf{Y}_j - \mathbf{Y}_{j-s}|}, & \text{OWA} &= \frac{1}{2} \left[\frac{\text{SMAPE}}{\text{SMAPE}_{\text{Naïve2}}} + \frac{\text{MASE}}{\text{MASE}_{\text{Naïve2}}} \right],
 \end{aligned}$$

where s is the periodicity of the time series, H is the prediction horizon, and \mathbf{Y}_h and $\hat{\mathbf{Y}}_h$ are the ground truth and prediction at time step h , respectively.

B. Complete results

B.1. Few-shot Forecasting

Table 11: Full few-shot learning results on 5% training data with forecasting horizons $H \in \{96, 192, 336, 720\}$. A lower value indicates better performance. ‘-’ means that 5% time series is not sufficient to constitute a training set. **Red**: the best, **Blue**: the second best

Methods	Time-VLM		Time-LLM		GPT4TS		DLinear		PatchTST		TimesNet		FEDformer		Autoformer		Stationary		ETSformer		LightTS		Informer		Reformer	
Metric	MSE	MAE	MSE	MAE	MSE	MAE	MSE	MAE	MSE	MAE	MSE	MAE	MSE	MAE	MSE	MAE	MSE	MAE	MSE	MAE	MSE	MAE	MSE	MAE	MSE	MAE
ETTh1	96	0.417 0.435	0.483 0.464	0.543	0.506	0.547	0.503	0.557	0.519	0.892	0.625	0.593	0.529	0.681	0.570	0.952	0.650	1.169	0.832	1.483	0.910	1.225	0.812	1.198	0.795	
	192	0.450 0.458	0.629 0.540	0.748	0.580	0.720	0.604	0.711	0.570	0.940	0.665	0.652	0.563	0.725	0.602	0.943	0.645	1.221	0.853	1.525	0.930	1.249	0.828	1.273	0.853	
	336	0.460 0.465	0.768	0.626	0.754	0.595	0.984	0.727	0.816	0.619	0.945	0.653	0.731 0.594	0.761	0.624	0.935	0.644	1.179	0.832	1.347	0.870	1.202	0.811	1.254	0.857	
	720	-	-	-	-	-	-	-	-	-	-	-	-	-	-	-	-	-	-	-	-	-	-	-	-	
Avg	96	0.442 0.453	0.627	0.543	0.681	0.560	0.750	0.611	0.694	0.569	0.925	0.647	0.658	0.562	0.722	0.598	0.943	0.646	1.189	0.839	1.451	0.903	1.225	0.817	1.241	0.835
	192	0.302 0.365	0.336 0.397	0.376	0.421	0.442	0.456	0.401	0.421	0.409	0.420	0.390	0.424	0.428	0.468	0.408	0.423	0.678	0.619	2.022	1.006	3.837	1.508	3.753	1.518	
	336	0.398 0.434	0.405 0.432	0.408	0.439	1.424	0.849	0.464	0.469	0.499	0.479	0.477	0.483	0.486	0.496	0.497	0.501	0.481	0.905	0.727	4.063	1.451	3.956	1.520	3.312	1.427
	720	-	-	-	-	-	-	-	-	-	-	-	-	-	-	-	-	-	-	-	-	-	-	-	-	
Avg	96	0.354 0.402	0.382 0.418	0.400	0.433	0.694	0.577	0.827	0.615	0.439	0.448	0.463	0.454	0.441	0.457	0.470	0.489	0.809	0.681	3.206	1.268	3.922	1.653	3.527	1.472	
	192	0.343 0.373	0.450	0.464	0.440	0.438	0.358	0.390	0.441	0.436	0.681	0.539	0.666	0.566	0.750	0.591	0.844	0.591	0.876	0.766	1.097	0.756	1.150	0.788	1.287	0.839
	336	0.373 0.391	0.450	0.424	0.485	0.459	0.402 0.416	0.499	0.467	0.786	0.597	0.807	0.628	0.851	0.659	0.870	0.603	1.138	0.787	1.147	0.775	1.198	0.809	1.288	0.842	
	720	0.425 0.420	0.483 0.471	0.577	0.499	0.511	0.489	0.767	0.587	0.796	0.593	0.822	0.633	0.857	0.655	0.893	0.611	1.245	0.831	1.200	0.799	1.175	0.794	1.247	0.828	
Avg	96	0.364 0.385	0.425	0.434	0.472	0.450	0.400 0.417	0.526	0.476	0.717	0.561	0.730	0.592	0.796	0.620	0.857	0.598	1.125	0.782	1.123	0.765	1.163	0.791	1.264	0.826	
	192	0.314 0.357	0.316 0.377	0.386	0.405	0.332	0.374	0.399	0.414	0.606	0.518	0.628	0.544	0.726	0.578	0.823	0.587	1.031	0.747	1.048	0.733	1.130	0.775	1.234	0.798	
	336	0.343 0.373	0.450	0.464	0.440	0.438	0.358	0.390	0.441	0.436	0.681	0.539	0.666	0.566	0.750	0.591	0.844	0.591	0.876	0.766	1.097	0.756	1.150	0.788	1.287	0.839
	720	0.425 0.420	0.483 0.471	0.577	0.499	0.511	0.489	0.767	0.587	0.796	0.593	0.822	0.633	0.857	0.655	0.893	0.611	1.245	0.831	1.200	0.799	1.175	0.794	1.247	0.828	
ETTh2	96	0.302 0.365	0.336 0.397	0.376	0.421	0.442	0.456	0.401	0.421	0.409	0.420	0.390	0.424	0.428	0.468	0.408	0.423	0.678	0.619	2.022	1.006	3.837	1.508	3.753	1.518	
	192	0.361 0.406	0.406 0.425	0.418	0.441	0.617	0.542	0.452	0.455	0.483	0.464	0.457	0.465	0.496	0.504	0.497	0.468	0.845	0.697	3.534	1.348	3.975	1.933	3.516	1.473	
	336	0.398 0.434	0.405 0.432	0.408	0.439	1.424	0.849	0.464	0.469	0.499	0.479	0.477	0.483	0.486	0.496	0.507	0.481	0.905	0.727	4.063	1.451	3.956	1.520	3.312	1.427	
	720	-	-	-	-	-	-	-	-	-	-	-	-	-	-	-	-	-	-	-	-	-	-	-	-	
Avg	96	0.354 0.402	0.382 0.418	0.400	0.433	0.694	0.577	0.827	0.615	0.439	0.448	0.463	0.454	0.441	0.457	0.470	0.489	0.809	0.681	3.206	1.268	3.922	1.653	3.527	1.472	
	192	0.343 0.373	0.450	0.464	0.440	0.438	0.358	0.390	0.441	0.436	0.681	0.539	0.666	0.566	0.750	0.591	0.844	0.591	0.876	0.766	1.097	0.756	1.150	0.788	1.287	0.839
	336	0.373 0.391	0.450	0.424	0.485	0.459	0.402 0.416	0.499	0.467	0.786	0.597	0.807	0.628	0.851	0.659	0.870	0.603	1.138	0.787	1.147	0.775	1.198	0.809	1.288	0.842	
	720	0.425 0.420	0.483 0.471	0.577	0.499	0.511	0.489	0.767	0.587	0.796	0.593	0.822	0.633	0.857	0.655	0.893	0.611	1.245	0.831	1.200	0.799	1.175	0.794	1.247	0.828	
ETTm1	96	0.314 0.357	0.316 0.377	0.386	0.405	0.332	0.242	0.171 0.224	0.207	0.253	0.229	0.230	0.277	0.299	0.215	0.252	0.218	0.295	0.230	0.285	0.497	0.497	0.406	0.435		
	192	0.224 0.298	0.215 0.275	0.256	0.316	0.306	0.373	0.264	0.324	0.311	0.361	0.394	0.361	0.291	0.357	0.298	0.349	0.347	0.479	0.521	3.578	1.475	3.553	1.484		
	336	0.282 0.338	0.273 0.330	0.318	0.353	0.380	0.423	0.334	0.367	0.338	0.366	0.378	0.427	0.478	0.517	0.353	0.380	0.552	0.555	1.415	0.879	3.561	1.473	3.446	1.460	
	720	0.375 0.397	0.433 0.412	0.460	0.436	0.674	0.583	0.454	0.452	0.509	0.465	0.523	0.510	0.553	0.538	0.475	0.445	0.701	0.627	1.822	0.984	3.896	1.533	3.445	1.460	
Avg	96	0.176 0.231	0.172 0.263	0.175	0.230	0.184	0.242	0.171 0.224	0.207	0.253	0.229	0.230	0.277	0.299	0.215	0.252	0.218	0.295	0.230	0.285	0.497	0.497	0.406	0.435		
	192	0.216 0.263	0.224 0.271	0.227	0.276	0.228	0.283	0.230	0.277	0.272	0.307	0.265	0.317	0.278	0.333	0.290	0.307	0.294	0.331	0.274	0.323	0.620	0.545	0.446	0.450	
	336	0.264 0.298	0.282 0.321	0.288	0.322	0.279	0.322	0.294	0.326	0.313	0.328	0.353	0.392	0.353	0.384	0.348	0.359	0.398	0.318	0.355	0.649	0.547	0.465	0.459		
	720	0.327 0.342	0.366	0.381	0.366	0.379 0.364	0.388	0.384	0.400	0.385	0.391	0.387	0.389	0.452	0.407	0.461	0.461	0.401	0.408	0.570	0.522	0.471	0.468	1.289	0.904	
ETTm2	96	0.185	0.296	0.147	0.242	0.244	0.214	0.150	0.251	0.145	0.244	0.131	0.189	0.138	0.235	0.192	0.247	0.148	0.286	0.129	0.283	1.265	0.919	1.414	0.855	
	192	0.194	0.302	0.158 0.241	0.159 0.255	0.163	0.263	0.163	0.260	0.138	0.196	0.124	0.247	0.141	0.241	0.135	0.257	0.127	0.272	0.128	0.289	1.240	0.919	1.414	0.855	
	336	0.210	0.315	0.178 0.277	0.179	0.274	0.175	0.278	0.183	0.281	0.140	0.245	0.126	0.267	0.151	0.256	0.135	0.274	0.127	0.289	1.302	0.942	1.253	0.921		
	720	0.251	0.346	0.224 0.312	0.233	0.323	0.215	0.209	0.233	0.323	0.163	0.259	0.147	0.277	0.161	0.264	0.147	0.278	0.126	0.289	1.259	0.919	1.249	0.921		
Avg	96	0.181	0.215																							

B.2. Zero-shot Forecasting

Table 13: Full zero-shot learning results on ETT datasets. A lower value indicates better performance.

Methods		Time-VLM		Time-LLM		LLMTime		GPT4TS		DLinear		PatchTST		TimesNet		Autoformer	
Metric		MSE	MAE	MSE	MAE	MSE	MAE	MSE	MAE	MSE	MAE	MSE	MAE	MSE	MAE	MSE	MAE
<i>ETTh1</i> \rightarrow <i>ETTh2</i>	96	0.277	0.338	0.279	0.337	0.510	0.576	0.335	0.374	0.347	0.400	0.304	0.350	0.358	0.387	0.469	0.486
	192	0.333	0.378	0.351	0.374	0.523	0.586	0.412	0.417	0.447	0.460	0.386	0.400	0.427	0.429	0.634	0.567
	336	0.360	0.399	0.388	0.415	0.640	0.637	0.441	0.444	0.515	0.505	0.414	0.428	0.449	0.451	0.655	0.588
	720	0.383	0.425	0.391	0.420	2.296	1.034	0.438	0.452	0.665	0.589	0.419	0.443	0.448	0.458	0.570	0.549
	Avg	0.338	0.385	0.353	0.387	0.992	0.708	0.406	0.422	0.493	0.488	0.380	0.405	0.421	0.431	0.582	0.548
<i>ETTh1</i> \rightarrow <i>ETTm2</i>	96	0.207	0.297	0.189	0.293	0.646	0.563	0.236	0.315	0.255	0.357	0.215	0.304	0.239	0.313	0.352	0.432
	192	0.258	0.329	0.237	0.312	0.934	0.654	0.287	0.342	0.338	0.413	0.275	0.339	0.291	0.342	0.413	0.460
	336	0.310	0.360	0.291	0.365	1.157	0.728	0.341	0.374	0.425	0.465	0.334	0.373	0.342	0.371	0.465	0.489
	720	0.398	0.412	0.372	0.390	4.730	1.531	0.435	0.422	0.640	0.573	0.431	0.424	0.434	0.419	0.599	0.551
	Avg	0.293	0.350	0.273	0.340	1.867	0.869	0.325	0.363	0.415	0.452	0.314	0.360	0.327	0.361	0.457	0.483
<i>ETTh2</i> \rightarrow <i>ETTh1</i>	96	0.434	0.441	0.450	0.452	1.130	0.777	0.732	0.577	0.689	0.555	0.485	0.465	0.848	0.601	0.693	0.569
	192	0.464	0.454	0.465	0.461	1.242	0.820	0.758	0.559	0.707	0.568	0.565	0.509	0.860	0.610	0.760	0.601
	336	0.489	0.481	0.501	0.482	1.328	0.864	0.759	0.578	0.710	0.577	0.581	0.515	0.867	0.626	0.781	0.619
	720	0.595	0.543	0.501	0.502	4.145	1.461	0.781	0.597	0.704	0.596	0.628	0.561	0.887	0.648	0.796	0.644
	Avg	0.496	0.480	0.479	0.474	1.961	0.981	0.757	0.578	0.703	0.574	0.565	0.513	0.865	0.621	0.757	0.608
<i>ETTh2</i> \rightarrow <i>ETTm2</i>	96	0.204	0.297	0.174	0.276	0.646	0.563	0.253	0.329	0.240	0.336	0.226	0.309	0.248	0.324	0.263	0.352
	192	0.255	0.328	0.233	0.315	0.934	0.654	0.293	0.346	0.295	0.369	0.289	0.345	0.296	0.352	0.326	0.389
	336	0.311	0.362	0.291	0.337	1.157	0.728	0.347	0.376	0.345	0.397	0.348	0.379	0.353	0.383	0.387	0.426
	720	0.420	0.425	0.392	0.417	4.730	1.531	0.446	0.429	0.432	0.442	0.439	0.427	0.471	0.446	0.487	0.478
	Avg	0.297	0.353	0.272	0.341	1.867	0.869	0.335	0.370	0.328	0.386	0.325	0.365	0.342	0.376	0.366	0.411
<i>ETTm1</i> \rightarrow <i>ETTh2</i>	96	0.297	0.356	0.321	0.369	0.510	0.576	0.353	0.392	0.365	0.415	0.354	0.385	0.377	0.407	0.435	0.470
	192	0.349	0.388	0.389	0.410	0.523	0.586	0.443	0.437	0.454	0.462	0.447	0.434	0.471	0.453	0.495	0.489
	336	0.374	0.409	0.408	0.433	0.640	0.637	0.469	0.461	0.496	0.494	0.481	0.463	0.472	0.484	0.470	0.472
	720	0.396	0.433	0.406	0.436	2.296	1.034	0.466	0.468	0.541	0.529	0.474	0.471	0.495	0.482	0.480	0.485
	Avg	0.354	0.397	0.381	0.412	0.992	0.708	0.433	0.439	0.464	0.475	0.439	0.438	0.457	0.454	0.470	0.479
<i>ETTm1</i> \rightarrow <i>ETTm2</i>	96	0.178	0.264	0.169	0.257	0.646	0.563	0.217	0.294	0.221	0.314	0.195	0.271	0.222	0.295	0.385	0.457
	192	0.226	0.298	0.227	0.318	0.934	0.654	0.277	0.327	0.286	0.359	0.258	0.311	0.288	0.337	0.433	0.469
	336	0.279	0.329	0.290	0.338	1.157	0.728	0.331	0.360	0.357	0.406	0.317	0.348	0.341	0.367	0.476	0.477
	720	0.373	0.385	0.375	0.367	4.730	1.531	0.429	0.413	0.476	0.476	0.416	0.404	0.436	0.418	0.582	0.535
	Avg	0.264	0.319	0.268	0.320	1.867	0.869	0.313	0.348	0.335	0.389	0.296	0.334	0.322	0.354	0.469	0.484
<i>ETTm2</i> \rightarrow <i>ETTh2</i>	96	0.285	0.347	0.298	0.356	0.510	0.576	0.360	0.401	0.333	0.391	0.327	0.367	0.360	0.401	0.353	0.393
	336	0.380	0.415	0.367	0.412	0.640	0.637	0.460	0.459	0.505	0.503	0.439	0.447	0.460	0.459	0.452	0.459
	720	0.424	0.451	0.393	0.434	2.296	1.034	0.485	0.477	0.543	0.534	0.459	0.470	0.485	0.477	0.453	0.467
	Avg	0.359	0.399	0.354	0.400	0.992	0.708	0.435	0.443	0.455	0.471	0.409	0.425	0.435	0.443	0.423	0.439
	Avg	0.370	0.390	0.359	0.397	1.179	0.781	0.747	0.558	0.570	0.490	0.491	0.437	0.747	0.558	0.735	0.576
<i>ETTm2</i> \rightarrow <i>ETTm1</i>	96	0.400	0.409	0.390	0.420	1.327	0.846	0.781	0.560	0.590	0.506	0.530	0.470	0.781	0.560	0.753	0.586
	192	0.426	0.420	0.421	0.443	1.478	0.902	0.778	0.578	0.706	0.567	0.565	0.497	0.778	0.578	0.750	0.593
	336	0.531	0.487	0.487	0.488	3.749	1.408	0.769	0.573	0.731	0.584	0.686	0.565	0.769	0.573	0.782	0.609
	720	0.432	0.426	0.414	0.438	1.933	0.984	0.769	0.567	0.649	0.537	0.568	0.492	0.769	0.567	0.755	0.591
	Avg	0.432	0.426	0.414	0.438	1.933	0.984	0.769	0.567	0.649	0.537	0.568	0.492	0.769	0.567	0.755	0.591

B.3. Short-term Forecasting

Table 14: Full short-term time series forecasting results. The forecasting horizons are in [6, 48] and the last three rows are weighted averaged from all datasets under different sampling intervals. A lower value indicates better performance.

Methods	Time-VLM	Time-LLM	GPT4TS	TimesNet	PatchTST	N-HiTS	N-BEATS	ETSformer	LightTS	DLinear	FEDformer	Stationary	Autoformer	Informer	Reformer	
Yearly	SMAPE	13.285	13.419	15.110	15.378	13.477	13.422	13.487	18.009	14.247	16.965	14.021	13.717	13.974	14.727	16.169
	MASE	2.993	3.005	3.565	3.554	3.019	3.056	3.036	4.487	3.109	4.283	3.036	3.078	3.134	3.418	3.800
	OWA	0.783	0.789	0.911	0.918	0.792	0.795	0.795	1.115	0.827	1.058	0.811	0.807	0.822	0.881	0.973
Quarterly	SMAPE	10.218	10.110	10.597	10.465	10.380	10.185	10.564	13.376	11.364	12.145	11.100	10.958	11.338	11.360	13.313
	MASE	1.203	1.178	1.253	1.227	1.233	1.180	1.252	1.906	1.328	1.520	1.350	1.325	1.365	1.401	1.775
	OWA	0.903	0.889	0.938	0.923	0.921	0.893	0.936	1.302	1.000	1.106	0.996	0.981	1.012	1.027	1.252
Monthly	SMAPE	12.788	12.980	13.258	13.513	12.959	13.059	13.089	14.588	14.014	13.514	14.403	13.917	13.958	14.062	20.128
	MASE	0.942	0.963	1.003	1.039	0.970	1.013	0.996	1.368	1.053	1.037	1.147	1.097	1.103	1.141	2.614
	OWA	0.886	0.903	0.931	0.957	0.905	0.929	0.922	1.149	0.981	0.956	1.038	0.998	1.002	1.024	1.927
Others	SMAPE	4.945	4.795	6.124	6.913	4.952	4.711	6.599	7.267	15.880	6.70					

B.4. Long-term Forecasting

Table 15: Full long-term forecasting results. We use the same protocol as in Table 1.

Methods	Time-VLM	Time-LLM	GPT4TS	DLinear	PatchTST	TimesNet	FEDformer	Autoformer	Stationary	ETSformer	LightTS	Informer	Reformer	
Metric	MSE	MAE	MSE	MAE	MSE	MAE	MSE	MAE	MSE	MAE	MSE	MAE	MSE	MAE
ETTh1	96	0.361 0.386	0.362 0.392	0.376	0.397	0.375	0.399	0.384	0.402	0.376	0.419	0.449	0.459	0.513
	192	0.397 0.415	0.398 0.418	0.416	0.418	0.405	0.416	0.413	0.421	0.436	0.429	0.420	0.448	0.500
	336	0.420 0.421	0.430 0.427	0.442	0.433	0.439	0.443	0.422	0.436	0.491	0.469	0.450	0.465	0.521
	720	0.441 0.458	0.442 0.457	0.477	0.456	0.472	0.490	0.447	0.466	0.521	0.500	0.506	0.507	0.514
Avg		0.405	0.420	0.408	0.423	0.465	0.455	0.422	0.437	0.413	0.430	0.458	0.450	0.440
ETTh2	96	0.267	0.335	0.268	0.328	0.285	0.342	0.289	0.353	0.274	0.336	0.340	0.374	0.358
	192	0.326	0.373	0.329	0.375	0.354	0.389	0.383	0.418	0.339	0.379	0.402	0.414	0.429
	336	0.357	0.406	0.368	0.409	0.373	0.407	0.448	0.465	0.329	0.380	0.452	0.452	0.496
	720	0.412	0.449	0.372	0.420	0.406	0.441	0.605	0.551	0.379	0.422	0.462	0.468	0.463
Avg		0.341	0.391	0.334	0.383	0.381	0.412	0.431	0.446	0.330	0.379	0.414	0.427	0.437
ETTm1	96	0.304	0.346	0.272	0.334	0.292	0.346	0.299	0.343	0.290	0.342	0.338	0.375	0.378
	192	0.332	0.366	0.310	0.358	0.332	0.372	0.335	0.365	0.332	0.369	0.374	0.387	0.426
	336	0.364	0.383	0.352	0.384	0.366	0.394	0.369	0.386	0.366	0.392	0.410	0.411	0.441
	720	0.402	0.410	0.383	0.411	0.417	0.421	0.425	0.421	0.416	0.420	0.478	0.450	0.543
Avg		0.350	0.377	0.329	0.372	0.388	0.403	0.357	0.378	0.351	0.380	0.400	0.406	0.448
ETTm2	96	0.160	0.250	0.161	0.253	0.173	0.262	0.167	0.269	0.165	0.255	0.203	0.287	0.255
	192	0.215	0.291	0.219	0.293	0.229	0.301	0.224	0.303	0.220	0.292	0.249	0.309	0.269
	336	0.270	0.325	0.271	0.329	0.286	0.341	0.281	0.342	0.274	0.329	0.321	0.351	0.325
	720	0.348	0.378	0.352	0.379	0.378	0.401	0.397	0.421	0.362	0.385	0.408	0.403	0.421
Avg		0.248	0.311	0.251	0.313	0.284	0.339	0.267	0.333	0.255	0.315	0.291	0.333	0.305
Weather	96	0.148	0.200	0.147	0.201	0.162	0.212	0.176	0.237	0.149	0.198	0.172	0.220	0.217
	192	0.193	0.240	0.189	0.234	0.204	0.248	0.220	0.282	0.194	0.241	0.219	0.261	0.276
	336	0.243	0.281	0.262	0.279	0.254	0.284	0.265	0.319	0.245	0.282	0.280	0.306	0.339
	720	0.312	0.332	0.304	0.316	0.326	0.337	0.333	0.362	0.314	0.334	0.365	0.359	0.371
Avg		0.224	0.263	0.225	0.257	0.237	0.270	0.248	0.300	0.225	0.264	0.259	0.287	0.309
Electricity	96	0.142	0.245	0.131	0.224	0.139	0.238	0.140	0.237	0.129	0.222	0.168	0.272	0.193
	192	0.157	0.260	0.152	0.241	0.153	0.251	0.153	0.249	0.157	0.240	0.184	0.289	0.201
	336	0.174	0.276	0.160	0.248	0.169	0.266	0.169	0.267	0.163	0.259	0.198	0.300	0.214
	720	0.214	0.308	0.192	0.298	0.206	0.297	0.203	0.301	0.197	0.290	0.220	0.320	0.246
Avg		0.172	0.273	0.158	0.252	0.167	0.263	0.166	0.263	0.161	0.252	0.192	0.295	0.214
Traffic	96	0.393	0.290	0.362	0.248	0.388	0.282	0.410	0.282	0.360	0.249	0.593	0.321	0.587
	192	0.405	0.296	0.374	0.247	0.407	0.290	0.423	0.287	0.379	0.256	0.617	0.336	0.604
	336	0.420	0.305	0.385	0.271	0.412	0.294	0.436	0.296	0.392	0.264	0.629	0.336	0.621
	720	0.459	0.323	0.430	0.288	0.450	0.312	0.466	0.315	0.432	0.286	0.640	0.350	0.653
Avg		0.419	0.303	0.388	0.264	0.414	0.294	0.433	0.295	0.390	0.263	0.620	0.336	0.624

C. Visualizations

C.1. Visualization of Generated Time Series Images

The image generation module employs advanced techniques—frequency and periodicity Encoding, multi-scale convolution, interpolation and normalization—to create informative and discriminative image representations of time series data. These representations enhance downstream VLMs for improved forecasting. As shown in Figure 5, the generated images capture key temporal characteristics through the following features:

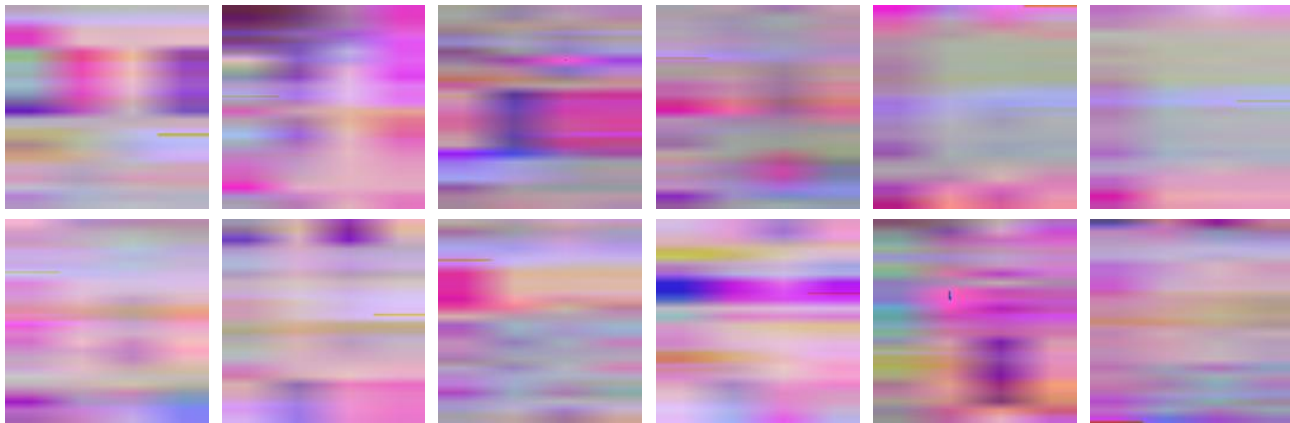


Figure 5: Time series transformed images, capturing key temporal characteristics, including trends, stationarity, seasonality, sudden changes, and frequency-domain patterns.

- **Frequency-Domain Information:** FFT integration captures frequency-domain characteristics, visualized as distinct textures—fine-grained for high-frequency components and broader color regions for low-frequency components.
- **Multi-scale Periodic Encoding:** Temporal dependencies at multiple scales (e.g., daily, weekly) are encoded, visible as regular patterns such as repeating vertical bands for daily cycles or broader horizontal patterns for weekly cycles.
- **Image Interpolation:** Bilinear interpolation ensures smooth and coherent images, preserving essential time series characteristics through seamless transitions between color intensities.
- **Color Trends:** Color intensity corresponds to time series values—darker regions (e.g., deep blue) indicate lower values, while brighter regions (e.g., yellow) represent higher values, enabling easy identification of trends.
- **Abrupt Changes and Anomalies:** Sudden shifts in color intensity (e.g., sharp transitions from dark to bright) highlight abrupt changes or anomalies, crucial for identifying irregular events like traffic spikes or weather shifts.

C.2. Visualization of prediction results

The prediction results in Figures 6, 7, 8, and 9 demonstrate Time-VLM’s ability to accurately forecast time series across diverse datasets and prediction horizons. For datasets with clear periodic structures, such as the daily cycles in ETTh1 and ETTm1, Time-VLM captures both global trends and fine-grained temporal patterns effectively. This is evident in the close alignment between the true values (solid lines) and predicted values (dashed lines) across all horizons. Similarly, for the ECL dataset, which exhibits regular consumption patterns, Time-VLM delivers highly accurate forecasts, showcasing its strength in handling structured environments.

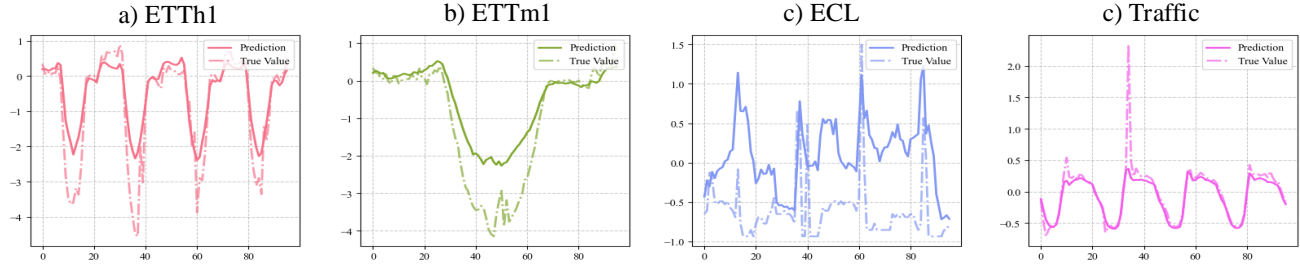


Figure 6: Prediction results visualization for ETTh1, ETTm1, ECL, and Traffic datasets at 96 prediction lengths. True values (solid line) and predicted values (dashed line) are shown for each dataset and horizon.

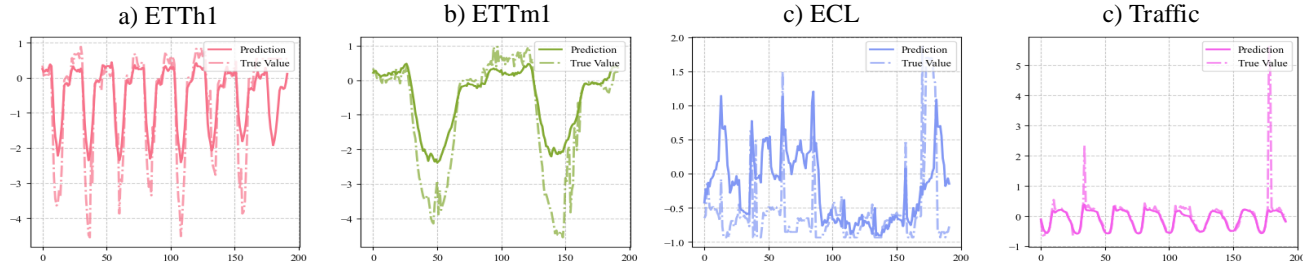


Figure 7: Prediction results visualization for ETTh1, ETTm1, ECL, and Traffic datasets at 192 prediction lengths. True values (solid line) and predicted values (dashed line) are shown for each dataset and horizon.

However, performance varies for datasets with irregular or abrupt changes. On the Traffic dataset, which is characterized by non-stationary patterns, Time-VLM shows slight deviations in capturing sudden fluctuations, particularly at longer horizons (e.g., 336 and 720). These deviations highlight the challenges of modeling highly irregular data and suggest opportunities for refining the time series-to-image transformation process to better handle such scenarios.

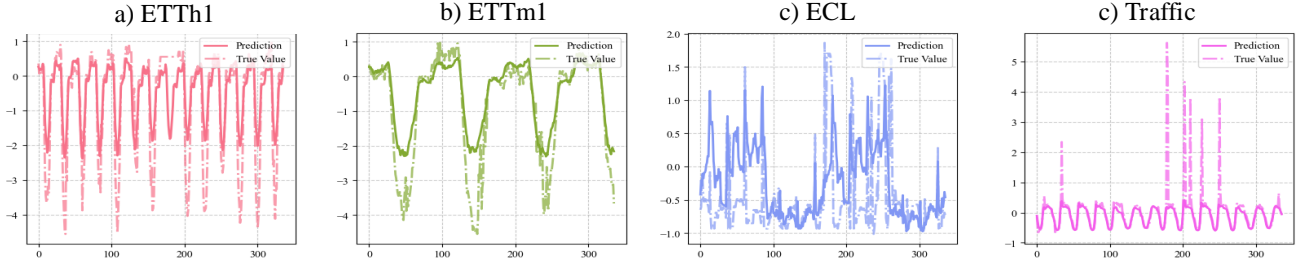


Figure 8: Prediction results visualization for ETTh1, ETTm1, ECL, and Traffic datasets at 336 prediction lengths. True values (solid line) and predicted values (dashed line) are shown for each dataset and horizon.

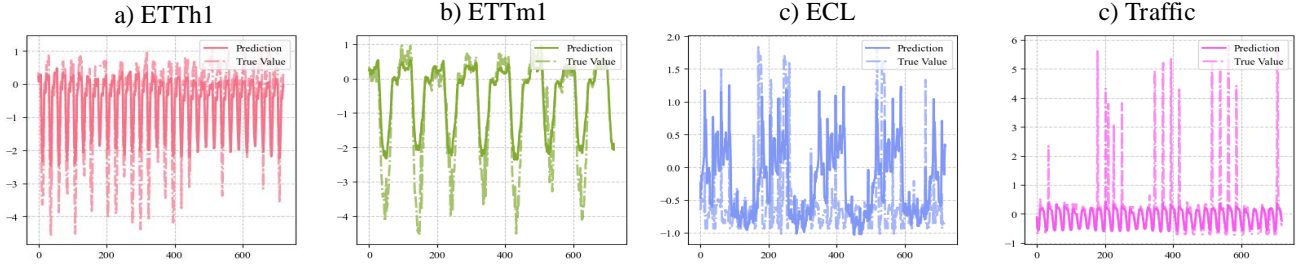


Figure 9: Prediction results visualization for ETTh1, ETTm1, ECL, and Traffic datasets at 720 prediction lengths. True values (solid line) and predicted values (dashed line) are shown for each dataset and horizon.

D. Future Work

D.1. Limitations

While Time-VLM demonstrates significant improvements in time series forecasting by integrating temporal, visual, and textual modalities, it has some limitations.

First, the framework performs less robustly on datasets with highly volatile or irregular patterns, such as those with sudden changes or non-stationary trends, compared to datasets with periodic structures. This limitation may arise from the current visual transformation techniques, which may not adequately capture abrupt temporal dynamics or sudden shifts. Future work could refine these transformations to better handle such irregularities.

Second, the current implementation relies on pre-trained VLMs like ViLT and CLIP, which are optimized for natural vision-language tasks rather than time series forecasting. While these models excel in visual understanding, their textual capabilities are limited, often supporting only shorter text inputs and lacking domain-specific knowledge relevant to time series. This restricts their ability to fully utilize textual context for forecasting. Future work could involve developing larger, domain-specific VLMs trained on multimodal time series datasets to address these limitations.

D.2. Future Work

Building on the current framework, several promising directions for future research emerge:

- **Optimizing Visual Transformations:** Future work could focus on developing adaptive visual transformation techniques that better preserve temporal dynamics, especially for datasets with irregular or non-stationary patterns, to more effectively highlight sudden changes and complex trends.
- **Scaling Multimodal VLMs for Enhanced Forecasting:** While the current framework uses smaller pre-trained Vision-Language Models (VLMs), scaling to larger models could improve forecasting accuracy. Investigating trade-offs between model size, computational efficiency, and performance is a promising direction for future research. Additionally, studying different VLM architectures could identify optimal designs for temporal modeling.
- **Interpretable Multimodal Learning for Time Series Analysis:** Understanding the contributions of visual and textual modalities in time series forecasting is crucial for improving model transparency. Future work could explore the

interpretability of multimodal features, analyzing how different types of information contribute to performance gains. This would provide deeper insights into temporal dependencies and enhance trust in multimodal forecasting models.

- **Pre-training Multimodal Foundation Models for Time Series Analysis:** Existing VLMs are not designed to handle time series data, limiting their ability to capture domain-specific temporal context. Future research could focus on constructing large-scale multimodal datasets that pair time series data with rich textual and visual annotations, enabling the development of models specifically optimized for time series forecasting. Additionally, this multimodal framework could be extended to support multi-task learning, enhancing the model's versatility for tasks such as anomaly detection, classification, or imputation. This would allow the model to capture a broader range of temporal patterns and dependencies, improving its applicability across various domains.

By addressing these directions, future research can build on the foundation laid by Time-VLM, advancing the field of multimodal time series forecasting while ensuring responsible and ethical deployment in real-world applications.